



Universiteit
Leiden
The Netherlands

Magnetism of a single atom

Otte, A.F.

Citation

Otte, A. F. (2008, March 19). *Magnetism of a single atom*. *Casimir PhD Series*. LION, AMC research group, Faculty of Science, Leiden University. Retrieved from <https://hdl.handle.net/1887/12660>

Version: Corrected Publisher's Version

License: [Licence agreement concerning inclusion of doctoral thesis in the Institutional Repository of the University of Leiden](#)

Downloaded from: <https://hdl.handle.net/1887/12660>

Note: To cite this publication please use the final published version (if applicable).

Chapter 1

^3He Scanning Tunneling Microscope Design

At school the bully always picks the smallest kid as his victim. That is because the amount of energy involved in displacing, rotating or deforming a small object is usually less than for larger objects. It is for this reason that Scanning Tunneling Microscopy and cryogenic temperatures form such a natural combination: as the physical scale of the object of study decreases, temperature needs to be reduced in order to keep the experiment controlled.

Today these two techniques are so well integrated that Scanning Tunneling Microscopes (STM's) operating at temperatures as low as 4 K in Ultra-High Vacuum (UHV) are commercially available in reliable and user-friendly configurations. While this temperature range is mostly sufficiently low to disable *atomic* motion, it is still too high for many studies of *electronic* behavior. For example, as we will see in the course of this thesis, electron spin excitations often occur at energies of only a few meV such that small variations cannot be discerned above ~ 1 K. Additionally, various fascinating macroscopic phenomena such as superconductivity and the Kondo effect in some situations have critical or typical temperatures that are well below 4 K. For the purpose of studying these and other situations it is desirable to further cool down an STM with help of liquid ^3He .

In this chapter we will discuss two experimental STM systems that are designed to operate at or below 500 mK in UHV, and are each equipped with a superconducting magnet that can generate a magnetic field up to 7 T or higher. Sections 1.1 through 1.3 give a detailed description of a set-up that is currently under construction in the Kamerlingh Onnes Laboratory in Leiden, based on an Oxford Instruments Heliox^{UHV} ^3He refrigerator. This system is very similar in design to the facility described in [21]. In section 1.4 we will more briefly review an existing system, located at the IBM Almaden Research Center in San Jose, CA, that was used for the experiments described in the remainder of this thesis.

1.1 Heliox^{UHV} ³He Refrigerator and Cryostat

During operation the Heliox^{UHV} ³He refrigerator shown in fig. 1.1, a commercial product of Oxford Instruments plc, is suspended within the UHV central tube of a ⁴He cryostat with liquid N₂ outer shield. The He dewar has a total capacity of 69 ℓ, however in order to guarantee the magnet to maintain its superconducting state, the effective volume is reduced to 51 ℓ. At standard boil-off rate, specified for this cryostat to be ≤ 0.83 ℓ/h, this corresponds to a hold time of at least 61 hours. The N₂ can, with 52 ℓ capacity, is specified to hold for 130 hours.

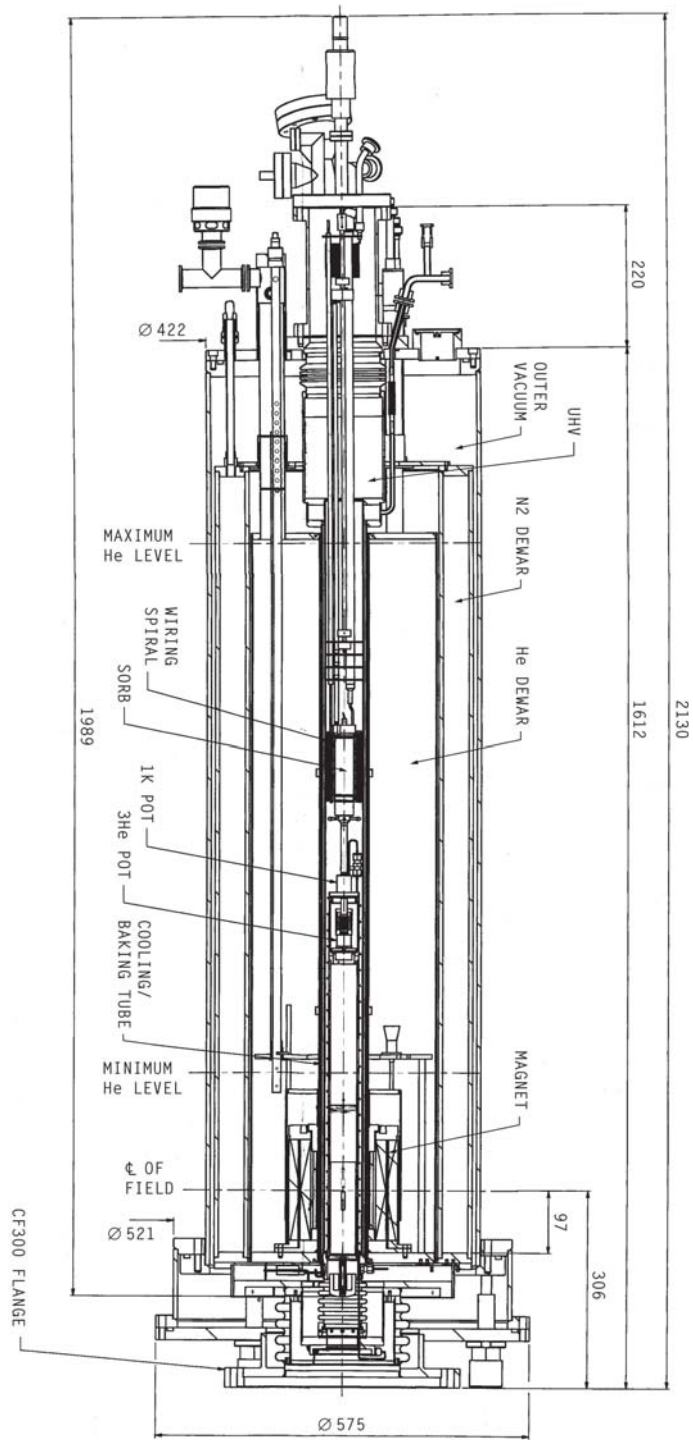
The superconducting magnet can generate a field of 10 T along the cryostat's vertical axis. Running the full current of 114 A through the dissipative leads (when ramping the field) gives rise to an additional 1.4 ℓ/h ⁴He boil-off. The size of the magnet's bore limits the central UHV tube to an inner diameter of 46 mm. The tube has a hollow wall through which liquid ⁴He can be pumped in order to cool it down to ~ 1.8 K, however, this only serves as a cold radiation shield and is not thermally coupled otherwise to the refrigerator.

1.1.1 Cooling Mechanism

Other than providing shielding, the cryostat does not directly cool the Heliox^{UHV} insert. Refrigeration occurs through a separate mechanism which is depicted schematically in fig. 1.2. The flow process can be divided into a ⁴He part and a ³He part, the latter of which is enclosed by a dashed line in the scheme.

We start with the ⁴He part. A spiralled capillary ("A") carries liquid helium from the bottom of the dewar to a 1K pot. Its flow can be regulated by an electrically driven needle valve mounted close to the beginning of the line. By an external pump the vapor above the liquid accumulated in the 1K pot is pumped through a second, much wider spiralled capillary ("B"). As a result the liquid in the pot cools down to ~ 1.8 K. During normal operation the needle valve is set to maintain a flow of approx. 4 ℓ/min gas through the pump (approx. 9 ℓ/min during initial cool down to 4.2 K). A bypass in the pumping line cools a sorption pump which is part of the ³He flow system. Additionally, there is a strong thermal coupling between the 1K pot and part of the ³He line. Except for radiation these are the only thermal connections between the two parts of the process.

Figure 1.1: (*Opposite page*) Technical drawing of the Heliox^{UHV} refrigerator and accompanying cryostat (cross-section). All dimensions in mm. The insert is drawn in its retracted position. A 1K shield, extending from the 1K pot down to the bottom of the 1989 mm insert length indicator, encompasses everything that should reach the 350 mK base temperature. Thereof only the ³He pot is part of the commercial assembly; the rest (i.e. STM head and suspension, not shown here) was built and developed in our laboratory. With the insert retracted and the suspension in its equilibrium position, the STM scanner is designed to have the junction in the central plane of the magnetic field. Reprinted with permission from Oxford Instruments plc.



In contrast to many comparable systems, in our case the ^3He part of the flow system has a linear configuration (rather than looped) and can therefore only be used in single-shot mode (as opposed to continuous flow mode). At the end of the line it has a 4.5ℓ ^3He reservoir originally filled to a pressure of 1 bar. During the initial cool down stage its gate valve is kept open such that the gas can freely roam through the line. As the 1K bypass cools the charcoal filled sorption pump (hereafter referred to as *sorb*) below approx. 40 K, ^3He gas becomes bound such that the pressure in the reservoir decreases. When the reservoir is (almost) empty, the gate valve is closed; now most gas is trapped in the sorb.

Next the sorb is gently heated to a temperature just above 40 K such that the gas is released and the pressure in the line increases. For safety a relief valve is fitted to allow gas back into the reservoir if the pressure exceeds 3.5 bar, although in practice it is easy to stay below this point. The ^3He now acts as a contact gas between the portion of the line that is linked to the 1K pot and the ^3He pot that is mounted below it, thus slowly cooling it down. When it reaches 3.2 K – depending on the heat load attached to the ^3He pot (e.g. the STM head, wiring etc.) this may take many hours – the gas starts to condense and liquid accumulates in the ^3He pot. After 30 to 60 minutes all gas has been condensed.

The final stage of the cooling procedure consists of switching off the sorb heater and tuning the 1K flow such that the sorb stays cold and acts as a pump. Eventually this cools down the liquid ^3He to its base temperature (approx. 350 mK). The hold time of this single-shot mode is approx. 20 hours, after which the ^3He should be recondensed by once more heating the sorb.

Throughout the process the temperature can be probed at various stations. The sorb is fitted with a 100Ω Allen-Bradley resistor thermometer (range 2 – 300 K), while the 1K pot temperature can be monitored by a $2.2 \text{ k}\Omega$ RuO_2 thick film resistor (range 20 mK – 8 K). The ^3He pot is equipped with one of each type (Allen-Bradley and RuO_2) such that the full range of operating temperatures is covered. Finally, in the housing of the STM scanner itself a CERNOXTM thermometer (range 300 mK – 100 K) is mounted. Additional heaters are installed on the 1K and ^3He pots to precisely regulate their temperatures if desired.

1.1.2 Large-Scale Assembly

At the bottom of the cryostat a CF300 flange (300 mm inner diameter, copper gasket sealed) connects to a home-built 420 mm deep UHV chamber that is pumped by a $300 \ell/\text{s}$ ion-pump. A pair of copper doors connected to the N_2 dewar thermally shield the refrigerator from room temperature radiation. Via an external motor drive unit the Heliox^{UHV} insert can be extended by 476 mm such that it reaches the bottom of the chamber. The radiation doors are pushed open by the insert and close automatically through a spring mechanism upon retracting the insert back into the cryostat. Using a manipulator stick the user can manually replace sample carriers (or tip carriers; in this STM system these are identical and interchangeable) on the STM scanner. In section 1.1.3 we will discuss how the scanner can be accessed for this operation.

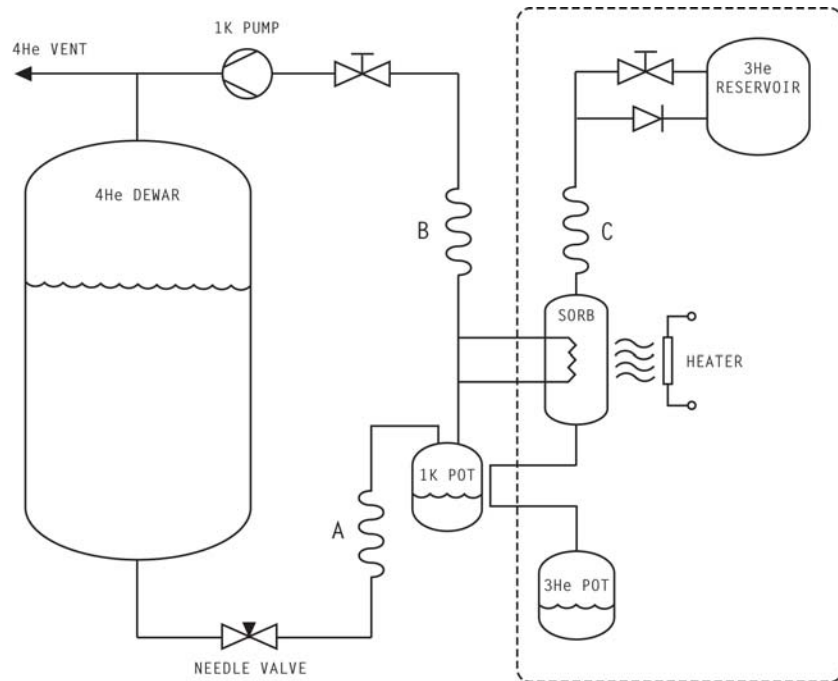


Figure 1.2: Flow diagram of the Heliox^{UHV} ³He refrigerator. The dashed line encloses the ³He part of the process to distinguish it from the ⁴He part. If the insert is extended in order to lower the STM into the main UHV chamber, spiral “A” is contracted whereas “B” and “C” are elongated.

In the main vacuum chamber up to 14 sample carriers can be stored in a fixed holder. Alternatively, samples can be transferred to a preparation chamber on a horizontal translator that can accommodate five carriers at once. Preparation techniques currently installed are a SPECS® IQE 11/35 ion-sputtering gun (0.2 – 5 kV) and a sample annealing station (approx. 600°C maximum). The preparation chamber additionally serves as a load-lock for adding new samples to the system and is pumped by a 60 ℓ/s turbo pump, which is also used for initial pumping of the total vacuum system (i.e. load-lock, main chamber, ion-pump and UHV part of cryostat).

The entire assembly is mounted in a rack that rests on four actively damped pneumatic pillars, two of which share one pressure regulator such that the system effectively rests on three points that move independently. The height of these points (i.e. the height of the top of the pillars) corresponds approximately to the height of the CF300 flange. The pillars stand on top of a separate ~ 10 tons concrete foundation, shared with one other experimental set-up, that is acoustically disconnected from the surrounding building.

1.1.3 Suspension and Access to the Scanner

Apart from the concrete foundation and the air-cushioned pillars there is a third step of vibration isolation. The STM head itself is attached to an approx. 25 cm long spring hanging freely below the ^3He pot. As shown in fig. 1.3, the spring hangs inside a gold-plated copper ^3He shield (that is named after the temperature it is supposed to assume). In order to ensure proper cooling of the scanner without creating an acoustic link, a copper ring is clamped to the inside of the shield. The suspension rod that holds the scanner assembly is connected to this ring by two bundles of approx. 250 flexible 0.05 mm \varnothing copper wires (not shown in the drawing to avoid cluttering) that are long enough not to generate any tension if the rod moves up or down.

Wires coming from the scanner pass through the copper ring and are then led through holes in the ^3He shield to proceed upward spiralling along the outside of the shield. Over a total length of approx. 35 cm they are glued onto the shield to provide a thermal anchor. For this purpose low vapor pressure glue is used, although as the shield is meant to be kept at cryogenic temperatures, contamination by degassing will in any case be strongly reduced.

The STM head, which will be described in detail in section 1.2, is mounted inside a 36 mm outer diameter gold-plated copper housing. After disconnecting all wires from the MACOR[®] connector plate, the entire housing can be easily removed from the suspension rod for repairs or alterations. Six ruby balls on the outside ensure that the contact area of the housing eventually touching the warmer shield around it is reduced to no more than a point. A threaded ring at the bottom of the housing is used to tightly clamp the scanner.

The 1K shield enveloping the parts mentioned above actually consists of two coaxial shields. The bottom of the outer shield is rounded for properly opening the N_2 -temperature radiation doors when the insert is lowered into the main chamber. This shape also acts as a ‘seeker’ when the insert reaches a metal cup it is supposed to rest in at the bottom of the chamber. In the center of this cup a rotatable ‘screwdriver’ protrudes upward that fits into a screw head that is part of the inner 1K shield. This stops the downward motion of the inner shield such that it rises with respect to the outer shield. As a result it pushes the STM scanner against the ^3He shield, which thus becomes fixed for transfer of sample carriers.

Both the inner and outer shields have windows that align vertically only if the inner shield is at its highest position with respect to the outer shield. By rotating the screwdriver the user can make them align horizontally as well. This provides access to the scanner for the manipulator stick. A spring between the two shields ensures that the window properly closes again once the insert is retracted into the cryostat. The screwdriver supporting the inner shield which in turn pushes the scanner against the ^3He shield creates a direct thermal connection between the ^3He pot and ambient temperatures. An experienced user can perform a complete tip and sample exchange in about 10 minutes. The heat that is thus introduced (through the screwdriver, the new sample carriers and radiation) necessitates an additional cooling time of several hours.

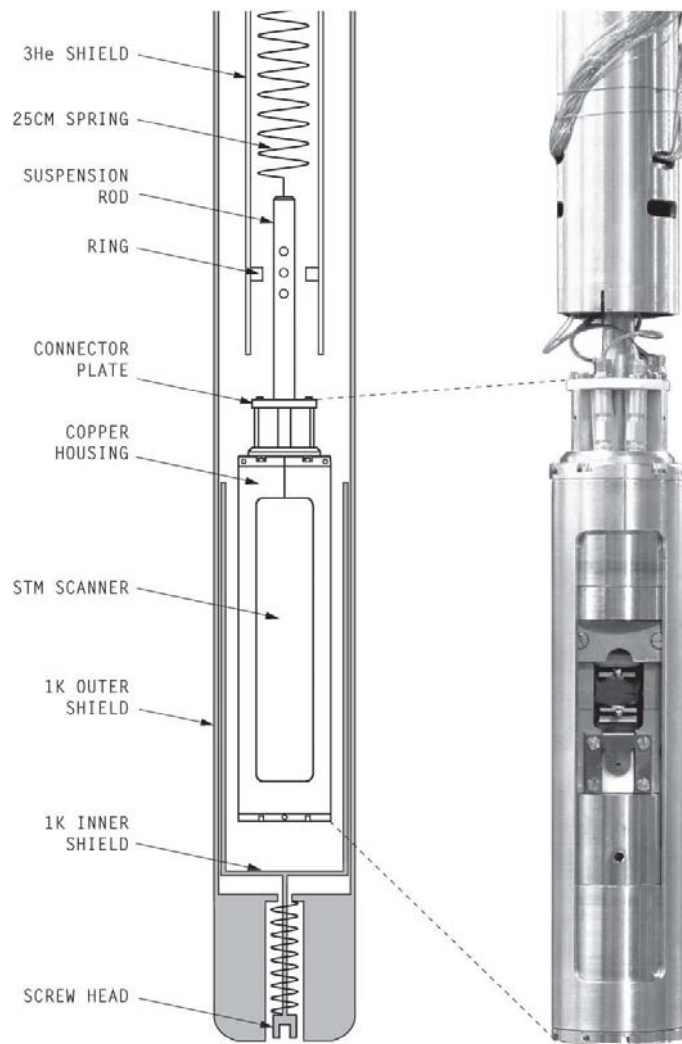


Figure 1.3: **Left:** Schematic drawing of the suspension of the STM scanner (not to scale). Parts that are colored white are thermally anchored to the ^3He pot, while grey parts are attached to the 1K pot. Bundles of copper wires connecting the suspension rod to the clamping ring, as well as the wires coming from the scanner are left out to avoid cluttering. **Right:** Photograph of the scanner mounted to the refrigerator. The 1K shields are not shown in the picture.

1.2 STM Head

¹ The STM head currently used is a home-built device with a walker-type coarse approach mechanism based on a design by Pan *et al.* [23], which is a reliable concept that is used in several comparable systems [21, 24]. Where most STM's of this type have a tube scanner mounted onto the slider that performs the scanning once the tip is in tunneling range, in the current design feedback is done by the same piezo actuators that are used for the coarse approach.

1.2.1 Walker Design

Figure 1.4 shows an expanded drawing of the assembly. Due to the dimensions of the copper housing mentioned in section 1.1.3 it is shaped as a 33 mm \varnothing cylinder. The main body is made of titanium for reasons of thermal expansion: in a design like this it is desirable to have all components expand roughly equally such that at any temperature all relative dimensions are the same. All piezo actuators used are stacked shear-elements from the PICATM-Shear series of PI Ceramic which have a coefficient of linear thermal expansion $\alpha = 4 - 8$ (in units of 10^{-6}K^{-1}) perpendicular to the polarization direction, whereas Ti has $\alpha = 8.6 \times 10^{-6}\text{K}^{-1}$.

Four X-shear piezo actuators² (3×3 mm, 5.5 mm high), each capped with a pad of aluminium-oxide (Al_2O_3), are glued onto the titanium body in two pairs that make an angle of 120° with each other. These support a 30 mm long prism-shaped walker (again made of titanium for the same reason), the sides of which have been polished and coated with titanium-carbide (TiC). Two additional X-shear actuators, identical to the others, are glued onto a small beam of MACOR[®] which is pushed down onto the walker by a 0.1 mm thick phosphorous-bronze leaf spring. To guarantee a point-like force at the center of the beam, a 1.5 mm \varnothing ruby ball is placed between the leaf spring and the beam. All actuators were glued into the assembly using STYCAST[®] 1266 A/B (a clear two-component epoxy). While baking the glue (1 hour at $60 - 70^\circ\text{C}$), the actual walker prism was used to apply pressure such that the surfaces would end up perfectly parallel ensuring maximum contact area.

Since the feedback (i.e. scan direction z) is taken care of by the same set of actuators, no tube scanner is required. Instead, a tip/sample station is glued directly onto the walker (separated by a thin MACOR[®] plate for insulation). Horizontal scanning (the x and y -directions) is done by a $10 \times 10 \times 9.5$ mm XY-shear stack glued onto a separable part of the body, also with a tip/sample station directly mounted onto it. Depending on whether the stations are occupied or not, the walker has a walking range of approx. 1.0 – 1.5 cm. In order to prevent a tip crash in case of the piezo stacks eventually losing grip on the walker the STM head is intended to be mounted with the XY-stack on top, although in principle it could work either way.

¹A general introduction into the principles of STM can be found in [22].

²Here the 'X' indicates that the piezo elements have only one direction of displacement as opposed to XY or XYZ-shear piezo actuators. It does not signify a specific direction in the coordinate frame of the scanner.

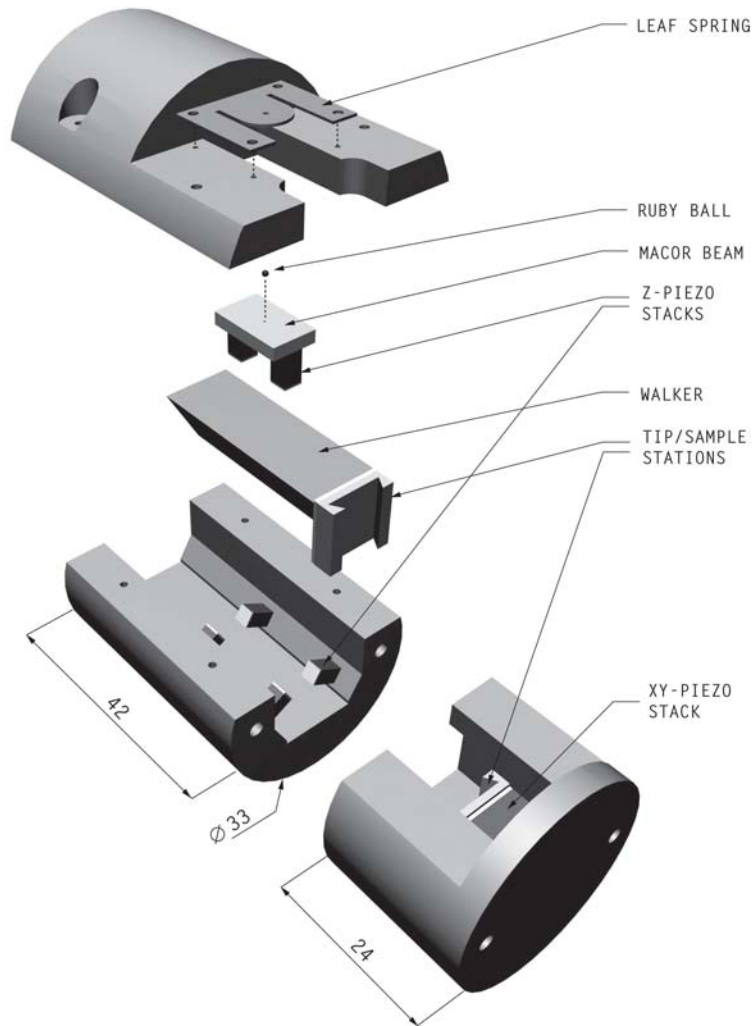


Figure 1.4: Expanded rendered drawing of the home-built Pan-design STM head. All dimensions in mm. The body, as well as the walker and the tip and sample stations are made of titanium; the walker is additionally coated with TiC. All piezo actuators are capped with an Al_2O_3 pad. The leaf spring consists of phosphorous-bronze. A thin insulating plate separates the walker electrically from the station glued onto it.

In figure 1.5 the sample mounting mechanism is demonstrated: a sample carrier fits onto a station through a dovetail joint (both are made of titanium). After sliding it in place it is pushed upward by a bent phosphorous-bronze leaf spring. This not only fixes the carrier but also ensures a strong thermal and electrical connection. A 9×9 mm object table provides ample space for

mounting samples, although only a very small portion of it can be scanned as no coarse movement in the x and y -directions is allowed for. Tip carriers are identical to sample carriers except for an additional 0.3 mm \varnothing hole in the center of the table. Tips mounted in the hole are fixed in place by a small screw in the body of the carrier.

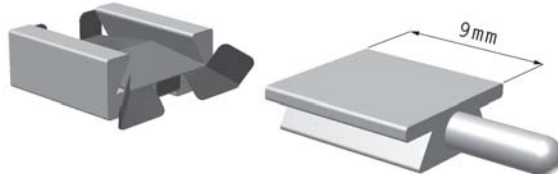


Figure 1.5: Sample station (left) and carrier, each made of titanium, form a dovetail joint. A phosphorous-bronze leaf spring holds the carrier in place.

1.2.2 Electronics and Dynamics

Two stainless steel coaxial cables run down from the top of the insert to the tip and sample electrodes. Spiralling down along capillary “B” of fig. 1.2, their length is set to approx. 6 m corresponding to a capacitance of 1.2 nF each. Directly at the top of the insert the measurement signal is amplified by a Stanford Research Systems Inc. SR570 pre-amplifier, which combined with the input impedance of the wires has a noise level of ~ 0.3 pA/ $\sqrt{\text{Hz}}$ at 10^{-9} A/V sensitivity. Feedback and scanning is performed by an RHK Technology Inc. SPM 100 controller with accompanying software.

Coarse Approach

The coarse approach piezo motor has been demonstrated to function properly at temperatures down to 350 mK in inertia-mode. In this mode all six piezo actuators are operated simultaneously. The actuators have a combined capacity of 8.6 nF and are specified to each have a total displacement of $3 \mu\text{m}$ ($\pm 30\%$) over a voltage range of 500 V at room temperature; at low temperature this reduces to approximately $0.35 \mu\text{m}$ (see section 1.3.2). They are driven by half parabola voltage pulses that in an automated approach are alternated by slow voltage ramps to check for tunneling current (see fig. 1.6); during the initial manual approach these are omitted to save time. Reliable values at low temperatures are 250 – 500 μs pulse width with an amplitude of 160 V, with a ramp of typically 200 V or higher amplitude and a few hundreds of milliseconds width. Here the leaf spring is bent such that the maximum friction force (i.e. the maximum force one can apply onto the walker before it starts to slide) at ambient conditions is between 0.5 and 0.8 N. At these settings the step size is such that several steps

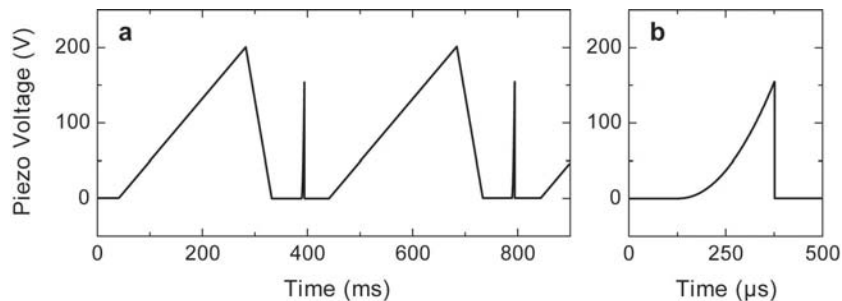


Figure 1.6: (a) Typical pulse train used for an automated approach, consisting of short driving pulses alternated with slow probing ramps. (b) Detailed plot of a driving pulse: a half parabola with a sharp cutoff. Reliable values are 160 V/250 μ s for the pulses, 200 V/200 ms for the ramps. Waiting times \gtrsim 10 ms.

(in the order of ten) fit in the walker’s total z -range. When moving downward the steps are larger than when moving upward by a factor of ~ 1.3 .

Manual approach can be performed while the insert is lowered such that there is visual access to the motor. Depending on how close the user brings the tip to the sample during this stage, the automated approach (performed after the insert has been retracted and the STM has cooled down) takes between 15 minutes and two hours. Between two measurements, e.g. while recondensing the ^3He , the tip is retracted by a few tens of steps such that experiments can be resumed almost immediately.

Walker Resonances

The scanner was designed to have high resonance frequencies in order to improve immunity against external vibrations. According to specifications the X-shear piezo stacks have their resonant frequency at 210 kHz. However, the walker assembly as a whole can have much lower-lying resonances. As these can seriously interfere with the feedback mechanism it is important to chart the motor’s vibrational spectrum. In fig. 1.7 we see such spectra in a range of 1 – 10 kHz; the upper curve corresponds to an ‘empty’ walker (total mass 6.87 g) while the lower was taken after mounting a 0.82 g sample carrier onto the walker. A strong resonance peak shifts downward from 8.4 tot 7.7 kHz upon placing the carrier and can therefore probably be assigned to a vibration mode of the system consisting of the walker being suspended by six piezo stacks. Here the ratio of the frequencies is 1.09 while the square root of the mass changes by a factor of 1.06. A weaker resonance occurs at 5.3 kHz in the upper curve which seems to split into multiple small peaks when the sample is loaded. Although it is more difficult to identify this mode, it could be related to the leaf spring being a free object in one case and becoming clamped in the other. In any case, no significant resonance takes place below an onset of 3.3 kHz which seems to be independent of the walker mass.

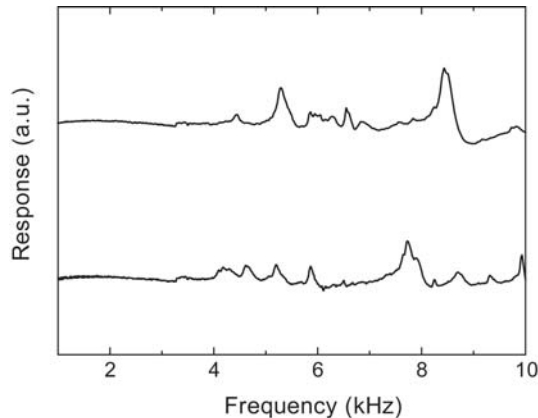


Figure 1.7: Resonance spectra of the six combined X-shear piezo stacks with (lower curve) and without (upper curve) a sample carrier mounted onto the walker, offset with respect to each other. Voltage response is measured over a $100\ \Omega$ resistor connected in series with the piezo elements, driven by a 1 V amplitude AC-signal at frequencies ranging from 1 to 10 kHz (measurements below 1 kHz did not show any resonances). From each curve a smooth background was subtracted. Before this measurement the maximum friction force of the walker was set to 0.75 N.

These resonances are not expected to cause any trouble during scanning. For example, images with a line-resolution of 512 data points can be scanned up to 6 Hz line-frequency before reaching the 3.3 kHz onset and even up to 15 Hz when only considering the main resonance.

1.3 Performance

Although the system is currently not yet fully operational, several test experiments have been performed for characterization and calibration purposes. Here we will review some of their results. All measurements presented were performed with a manually cut 0.25 mm \varnothing platinum-iridium tip (90% Pt, 10% Ir).

1.3.1 Superconducting Gap

The actual temperature of a tunnel-junction can be studied very well using a superconducting sample. For this purpose an α - $\text{Mo}_{2.7}\text{Ge}$ film, covered with a thin gold capping layer, was mounted in the scanner and cooled down. α - $\text{Mo}_{2.7}\text{Ge}$ is a type II superconductor, the critical temperature T_c of which depends strongly on the film thickness d , but saturates around 6.3 K for $d \gtrsim 40$ nm [25]. Measurements of the differential conductance dI/dV were performed at various temperatures, two of which are shown in fig. 1.8: at 2.5 K and 400 mK as indicated on the thermometer that is mounted in the body of the STM head (the latter value corresponds to the base temperature of 350 mK on the ^3He pot).

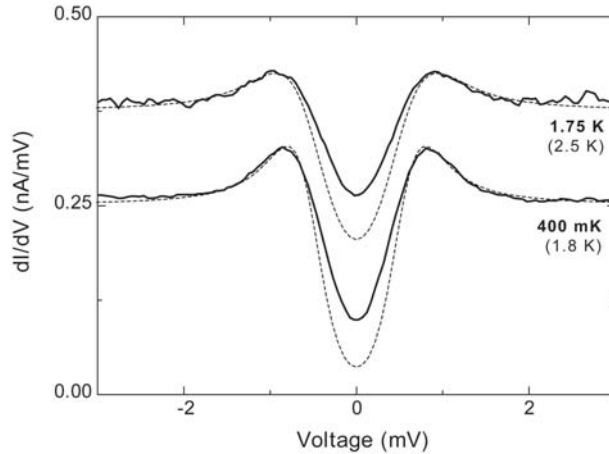


Figure 1.8: Conductance spectra taken on a Au-capped α -Mo_{2.7}Ge film at 1.75 K and 400 mK (as indicated by the thermometer mounted in the STM head) at 80 mV/20 nA quiescent settings. The upper curve is offset by 0.125 nA/mV for clarity. Measurements were performed by lock-in technique (100 μ V AC-modulation at 716 Hz, 20 mV sensitivity, 30 ms integration time). The smooth dashed lines are thermally broadened BCS densities of states at effective temperatures of 2.5 and 1.8 K, manually fitted to the shape of the peaks (rather than to the gap).

The spectra were fitted by hand using the Bardeen-Cooper-Schrieffer (BCS) density of states [26],

$$\frac{\rho_{\text{BCS}}(\varepsilon)}{\rho_0} = \begin{cases} \frac{\varepsilon}{\sqrt{\varepsilon^2 - \Delta^2}} & \text{if } \varepsilon > \Delta, \text{ and} \\ 0 & \text{if } \varepsilon < \Delta, \end{cases} \quad (1.1)$$

being broadened with an effective temperature T_{eff} (see section 4.2.1 for details on thermal and modulation broadening). In the above expression ε is the energy and Δ half the width of the energy gap. The parameters Δ and T_{eff} were manually adjusted to obtain a best fit, resulting in $\Delta = 0.55$ meV for both spectra and $T_{\text{eff}} = 2.5$ and 1.8 K for the high and low-temperature measurements respectively. Using the expression $\Delta = 1.76k_B T_c$ (k_B is Boltzmann’s constant), which applies fairly well for $T \lesssim T_c/2$ [26], we find $T_c = 3.6$ K, corresponding to a layer thickness $d \simeq 10$ nm.

These high effective temperatures can be partly explained by the 0.1 mV AC-modulation signal added to the voltage for lock-in detection, resulting in an extra ‘modulation temperature’ $T_{\text{mod}} = 0.9$ K. Subtracting this we find actual temperatures $T = \sqrt{T_{\text{eff}}^2 - T_{\text{mod}}^2} = 2.3$ and 1.6 K respectively, which are still rather high. Two principal candidates for the source of this discrepancy are (1) inadequate thermal anchoring of tip and sample and (2) insufficient filtering of RF-noise leaking in through the leads.

1.3.2 Piezo Calibration

The x and y scan motions were calibrated by imaging the surface of a highly oriented pyrolytic graphite (HOPG) sample. In fig. 1.9 two images are shown, taken at 600 mK and 2 K. Although technically the 2 K results were used for calibration, sensitivity of the piezo-elements hardly varies at these temperatures. Large scale images such as the one on the left did not show any defects in the

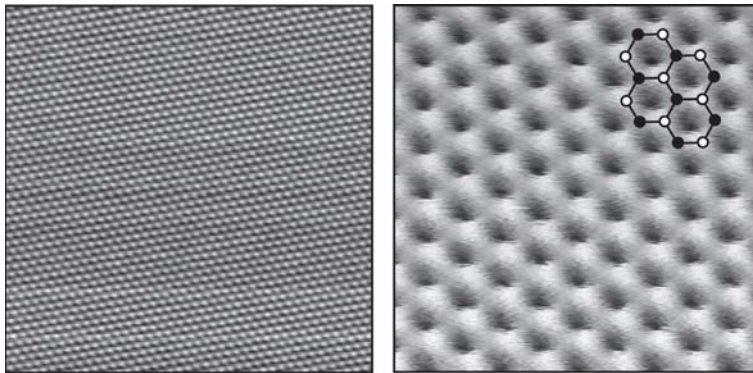


Figure 1.9: STM images of HOPG at 600 mK (**left**, 10×10 nm) and 2 K (**right**, 2×2 nm), recorded with 0.8 V/40 nA. The apparent height is represented in greyscale, with a maximum difference of approx. 5 Å. The overlay on the right image suggests a possible hexagonal lattice assignment.

hexagonal pattern. This might result from scanning with a non-ideal, multiple tip [22]. However, as several independent measurements at portions of the graphite surface with different orientations all produced equal lattice spacings, it is unlikely that the observed patterns result from mere interference between the sample and an eventual flake of graphite on the tip. Also, the resulting piezo calibration of 7.0 Å/V (both for the x and y -directions) agrees reasonably well with the specified sensitivity: 6 nm/V ($\pm 30\%$) at room temperature. With a voltage range of 500 V this gives a total low-temperature scan range of 350×350 nm.

On the right image an overlay indicates a possible identification of the lattice. Here carbon atoms from one sublattice (white circles) appear more brightly than those from the other sublattice (black), resulting from a variation in the local density of states. The correct assignment might be shifted with respect to the presented one, but both the scale and the orientation should be accurate.

Proper calibration of the z -motion, on a stepped surface with a known step height, has currently not yet been performed at low temperatures. However, as the X-shear actuators that move the walker are made of the same piezo-ceramic material as the XY-shear stack that is used for horizontal scanning, we can as a first approximation assume an equal reduction in sensitivity upon cooling down to cryogenic temperatures. This again results in 7.0 Å/V, or a total range of 0.35 μm as suggested in section 1.2.2.

1.3.3 Tentative Assessment

The ^3He STM system described in these first three sections is in an advanced stage of its development. Judging from the successes on an almost identical system [21] it is based on a design that has proven itself and each of the individual components has at some point functioned properly. However, several weaknesses have been detected during the assemblage and testing stages.

- The **1K capillary**, transporting ^4He from the dewar to the 1K pot, has developed leaks into the UHV chamber on multiple occasions. On either end (i.e. at the dewar and at the 1K pot) it is connected by a SWAGELOK VCR[®] fitting, which requires a considerable torque for proper sealing. Since one of these has to be resealed every time the insert is removed from the cryostat, the capillary is permanently at risk of being weakened until it rips.
- Similarly the **^3He capillary**, spiralling down to the sorb, is a notorious source of trouble. Made of copper-nickel, its wall is quite fragile. Repeatedly extending and retracting the insert can cause it to kink, with a blockage as result. It cannot be easily accessed for repairs and once reached it is very difficult to mend reliably. Opening the line leads to expensive ^3He losses and contamination of the sorption pump.
- The **vertical motion mechanism** for lowering the insert into the main chamber has failed several times. It consists of a rotating threaded rod along which a nut (that holds the weight of the entire insert) can move up or down. Friction wears the thread inside the nut until it fails after only tens of runs. MoS_2 powder is supposed to prevent this, but the rod cannot be easily accessed for replenishing the lubricant.

Each of these problems in itself can in principle be evaded by careful handling, but together they cumulatively reduce the chance of a successful measurement and thus weaken the design. In a scientific instrument that is intended to operate at and beyond the boundaries of technology we cannot afford those components that rely on conventional technology to be less than optimal.

All of the issues listed above are in a sense related to the fact that the cryostat is ‘bottom-loaded’: in order for samples to be replaced the entire refrigerator has to move through the vacuum and therefore everything has to be flexible and fragile. Mechanical motion should be avoided as much as possible, especially when the choice of materials is limited by the requirements of UHV and low-temperature compatibility.

The alternative is to make the cryostat accessible from top, such as the system briefly reviewed in the next section. This way the cooling mechanism can remain fixed and only the STM head (or even only the sample) is picked up and transferred to the main chamber above if desired. As an additional advantage, having the He dewar below the suspension enhances stability by lowering the center of mass, not to mention obviating the discomforts and hazards of having to refill a 3 m tall column with liquid helium.

1.4 Joule-Thomson Refrigerated ^3He STM

Built by A.J. Heinrich and coworkers, the ^3He STM system located at the IBM Almaden Research Center is inspired by an earlier design for a 4 K STM by D.M. Eigler. In this top-loaded construction, the scanner assembly permanently stays down in the cryostat while samples can be transferred to and from the preparation chamber via an ~ 150 cm long manipulator rod connected to an almost equally long UHV bellow (tip exchange is currently precluded).

In contrast to many other ^3He refrigerators, here the ^3He gas is cooled by the Joule-Thomson effect [27]. The UHV area, protruding down from the main chamber along the central axis of the cryostat, ends with a glass tube at the bottom of which the STM head is mounted. This glass tube hangs inside an exchange gas can, which is part of a closed ^3He cooling cycle. Gas expands into the can through a nozzle and is pumped through a much wider line, until it condenses and accumulates as a liquid at the bottom of the can. Note that in this system no ^4He -filled 1K pot is required. Other than cooling the superconducting magnet, the only purpose of the ^4He dewar around the can is to serve as a 4.2 K thermal shield.

Three modes of operation can be distinguished:

1. In **static mode**, the can is filled with static ^3He gas (i.e. nozzle and pumping line are closed), thermally linking the He dewar to the STM which thereby equilibrates to 4.2 K.
2. In **continuous-flow mode** the gas is cooled by Joule-Thomson expansion as discussed above. Both the nozzle and the pumping line are opened. This eventually results in a temperature of 1.4 K.
3. Finally the supply of new warm gas can be stopped by closing the nozzle. When being run in this **single-shot mode**, the system can reach 0.5 K.

Using an additional heater mounted in the STM head, intermediate temperatures can be realized, at least on the sample. As a result of the design, both the heater and the thermometer attached to the scanner are strongly coupled to the sample station but hardly to the tip, which is cooled almost directly by the liquid ^3He .

The cryostat is equipped with a superconducting 7 T split-coil magnet. Its field is oriented perpendicular to the cryostat's axis (i.e. horizontal). The field orientation within the horizontal plane can in principle be chosen freely, but is fixed once the cryostat is mounted in place. As the STM head is designed such that the sample stands upright (apart from a $\sim 7^\circ$ tilt), the magnetic field can be oriented either perpendicular or parallel to the sample surface. Switching from one situation to the other involves warming up the system and dismounting the dewar and cannot be done without having to prepare the sample anew.

All experiments presented in the remainder of this thesis were performed on this instrument.